Journal of Organometallic Chemistry, 417 (1991) 407–420
Elsevier Sequoia S.A., Lausanne

JOM 21968

EPR studies of photochemical reactions of $[MeCpMo(CO)_3]_2$ with quinones

Minoru Hanaya [1] and Masamoto Iwaizumi *

Chemical Research Institute of Non-Aqueous Solutions, Tohoku University, Katahira 2, Aoba-ku, Sendai 980 (Japan)

(Received January 18th, 1991)

Abstract

The photochemical reactions of hexacarbonylbis[(1,2,3,4,5-η)-1-methyl-2,4-cyclopentadien-1-yl]dimolybdenum (**2**) and *o*-quinones, 1,2-diketones and *p*-benzoquinones have been investigated by EPR spectroscopy. The reactions proceed in the same way as in the case of hexacarbonylbis(η^5-2,4-cyclopentadien-1-yl)dimolybdenum (**1**) as previously reported, but the observed paramagnetic products differ in characteristic features from the complexes derived from **1**. As in the case of **1**, the paramagnetic products of **2** with *o*-quinone or 1,2-diketone ligands show appreciable changes of *g* values and Mo hyperfine couplings with the ligands, reflecting the changes in the spin distribution between the metal fragment and the ligands but in general in complexes from **2** the unpaired spin tends to delocalize more onto the metal fragment. The presence of the isomers (which have different orientation of the methyl group in the cyclopentadienyl ring) was inferred from the line width broadening in the EPR spectra. The methyl group in the cyclopentadienyl ring affects the preference of the carbonyl group which coordinates to the metal to a greater extent in the coordination of substituted *p*-benzoquinones. A remarkable temperature dependence of the EPR spectra has been observed in the complexes of **2** with *p*-benzoquinones. The intramolecular motions and the most stable conformation of the quinone ligand in such a complex are discussed based on the spectra.

Introduction

There have been extensive studies on the photochemical reactions of metal carbonyl complexes containing a metal–metal bond, because the molecules display fascinating and diverse photochemical properties. Photoirradiating the complexes in solutions commonly effects homolytic cleavage of the metal–metal bond, and the resulting paramagnetic species undergo various reactions [1–4].

We have previously reported that photoirradiating hexacarbonylbis(η^5-2,4-cyclopentadien-1-yl)dimolybdenum, $[CpMo(CO)_3]_2$ (**1**) in the presence of *o*-quinones or 1,2-diketones yields paramagnetic complexes of the type of $CpMo(CO)_2$-

---

[1] Present address: Department of Chemistry, Faculty of Science, Tokyo Institute of Technology, O-okayama 2, Meguro-ku, Tokyo 152, Japan.

(o-quinone) containing the o-quinone or the 1,2-diketone as a bidentate ligand, which show interesting patterns of spin distribution [5], while photoirradiation in the presence of p-benzoquinones yields paramagnetic complexes of the type $CpMo(CO)_3$(p-benzoquinone) containing the p-benzoquinone as a monodentate ligand [6]. In the present work, we report the study of photochemical reactions of hexacarbonylbis[(1,2,3,4,5-η)-1-methyl-2,4-cyclopentadien-1-yl]dimolybdenum, $[MeCpMo(CO)_3]_2$ (**2**), with o-quinones, 1,2-diketones, and p-benzoquinones to obtain further information about the photochemical reactions of the molybdenum carbonyl complexes with quinones and the structures of the paramagnetic complexes thus produced.

Experimental section

$[MeCpMo(CO)_3]_2$ (**2**) was obtained from Strem Chemicals and used as received. $[MeCpMo(^{13}CO)_3]_2$ (**2′**) was synthesized from **2** by the photosubstitution of CO with ^{13}CO under a ^{13}CO atmosphere [7–10] in toluene. 1,2-Acenaphthenequinone (AQ) and 9,10-phenanthrenequinone (PQ) were vacuum sublimated before use. 1-Phenyl-1,2-propanedione (PPD) and diacetyl (DA) were vacuum distilled. Furyl (FR) and benzyl (BZ) of the best commercially available grade were used without further purification. 1,4-Benzoquinone (BQ), 2-methyl-1,4-benzoquinone (2-DMBQ), 2,5-di-tert-butyl-1,4-benzoquinone (2,5-DBBQ), and 2-phenyl-1,4-benzoquinone (2-PBQ) were purified by sublimation. 2,6-Dimethyl-1,4-benzoquinone (2,6-DMBQ), 2,5-dimethyl-1,4-benzoquinone (2,5-DMBQ), 2,6-di-tert-butyl-1,4-benzoquinone (2,6-DBBQ), 2,5-diphenyl-1,4-benzoquinone (2,5-DPBQ), 2,3,5,6-tetrafluoro-1,4-benzoquinone (TFBQ), and 2,3,5,6-tetrachloro-1,4-benzoquinone (TCBQ) of the best commercially available grade were used without further purification.

Toluene for use as a solvent was purified and dried by distillation over molecular sieves *in vacuo*. Tetrahydrofuran (THF) and 2-methyltetrahydrofuran (MTHF) were

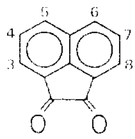

AQ

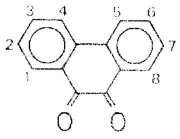

PQ

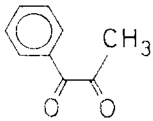

PPD

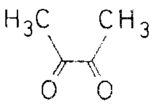

DA

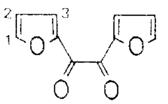

FR

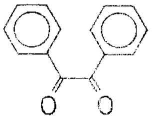

BZ

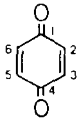
BQ

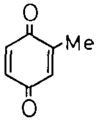
2-MBQ

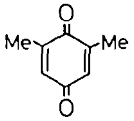
2,6-DMBQ

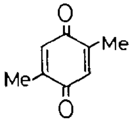
2,5-DMBQ

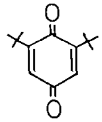
2,6-DBBQ

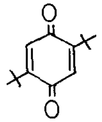
2,5-DBBQ

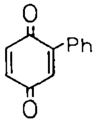
2-PBQ

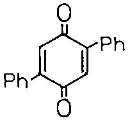
2,5-DPBQ

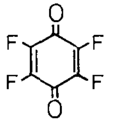
TFBQ

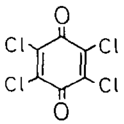
TCBQ

purified by distillation from $LiAlH_4$ under nitrogen atmosphere and stored with the sodium perylene anion and sodium benzophenone ketyl anion, respectively. In preparation of samples for EPR measurements, these solvents were distilled through a vacuum line to a vessel containing the reagents. Typical sample solutions containing 2 (1 mg) and the quinones (1 mg) in ca. 1 cm^3 of toluene were prepared in a vessel connected to a 5 mm o.d. quartz EPR tube. The solutions were degassed on the vacuum line and kept at the liquid nitrogen temperature until just before photolysis. The solution in the quartz tube was irradiated *in situ* in an EPR cavity with a 100 W high pressure mercury lamp equipped with a UV filter (< 310 nm) and a remote controlled shutter at or below room temperature.

In the experiments with *p*-benzoquinones, THF and MTHF were also used as solvents, and for measurements at lower temperatures, MTHF was used instead of toluene since MTHF solutions gave better spectral resolution at low temperatures because of their lower viscosity.

EPR spectra were recorded on a Jeol JES-FE2XG X-band spectrometer. The temperature was controlled by the standard accessories. The microwave frequency was monitored with a Takedariken TR5501 frequency counter equipped with a TR5023 frequency converter. The magnetic fields were measured with an Echo electronics EFM2000 NMR oscillator and the magnetic field difference between the NMR probe and sample positions was calibrated by DPPH.

Results and discussion

Photochemical reaction of $[MeCpMo(CO)_3]_2$ (**2**) with *o*-quinones and 1,2-diketones. The toluene solution containing **2** and AQ showed an EPR spectrum after photoirradiation at room temperature which exhibited the hyperfine (hf) splittings

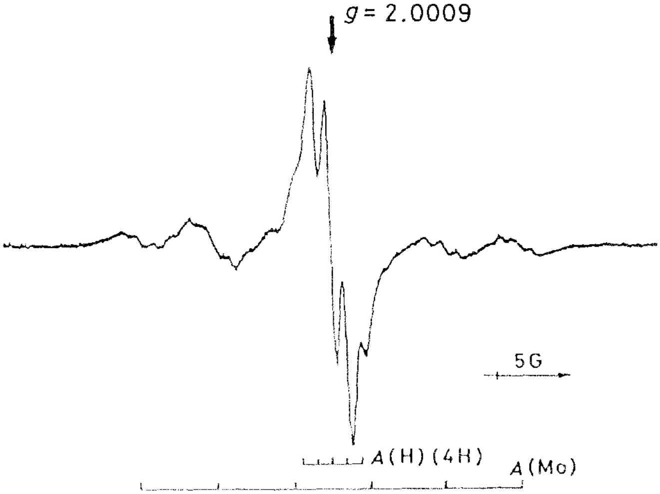

Fig. 1. First-derivative X-band EPR spectrum observed after photoirradiation at room temperature of a toluene solution containing **2** and AQ.

arising from the interaction with the AQ protons and the satellite lines due to the interaction with the magnetic isotopes ^{95,97}Mo ($I = 5/2$) (Fig. 1). When the ^{13}CO enriched **2′** was used instead of **2**, an additional triplet hf splitting due to the two equivalent ^{13}C's ($I = 1/2$) was observed (Fig. 2). As in the case of **1** [5], the spectrum can be assigned to the paramagnetic complex of the type of MeCpMo(CO)$_2$(AQ) having a chelate structure of AQ.

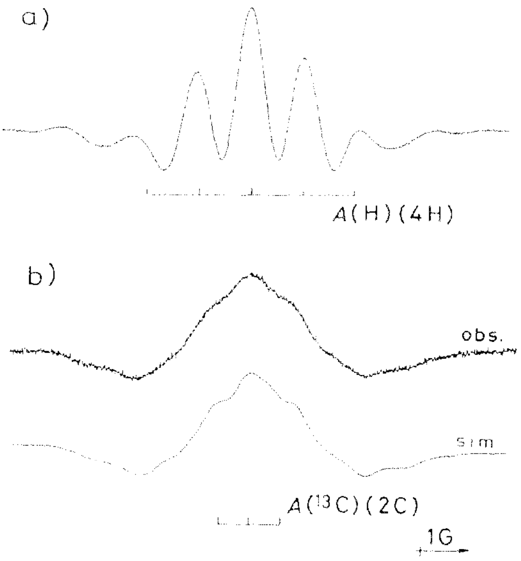

Fig. 2. Second-derivative X-band EPR spectra observed after photoirradiation at room temperature of toluene solutions containing AQ and **2** (a) or **2′** (b) and the simulated spectrum of b.

Table 1

EPR parameters for the paramagnetic complexes and the anion radicals of *o*-quinones and 1,2-diketones

o-Quinone or 1,2-diketone	Metal or counter ion	Solvent	*g* value	a_{Mo}/G	a_H/G [a]
PQ	$MeCpMo(CO)_2$	toluene	1.9964	11.7	$a_H1,3,6,8 = 1.0$ (4H)
					$a_{13C} = 2.1$ (2C) [b]
	$CpMo(CO)_2$ [c]	toluene	1.9957	11.2	$a_H1,3,6,8 = 1.0$ (4H)
					$a_{13C} = 1.9$ (2C) [b]
	$(^nBu)_4N^+$	DMF [d]	2.0049	–	$a_H3,6 = 1.67$ (2H)
					$a_H1,8 = 1.34$ (2H)
					$a_H4,5 = 0.42$ (2H)
					$a_H2,7 = 0.21$ (2H)
	$MeCpMo(CO)_3$ [e]	toluene	2.0051	–	$a_H1,3 = 2.5$ (2H)
					$a_H2,4,6,8 = 0.8$ (4H)
	$CpMo(CO)_3$ [f]	toluene	2.0050	–	$a_H1 = 2.63$ (1H)
					$a_H3 = 2.37$ (1H)
					$a_H2,4,6,8 = 0.8$ (4H)
					$a_{13C} = 0.75$ (1C) [b]
FR	$MeCpMo(CO)_2$	toluene	1.9983	9.1	$a_H1,3 = 1.0$ (4H)
	$CpMo(CO)_2$ [c]	toluene	1.9975	8.6	$a_H1.3 = 1.2$ (4H)
	$(^nBu)_4{}^+$	DMF [d]	2.0048	–	$a_H3 = 2.0$ (2H)
					$a_H1 = 1.5$ (2H)
					$a_H2 = 0.35$ (2H)
Bz	$MeCpMo(Co)_2$	toluene	1.9986	9.0	–
	$CpMo(CO)_2$ [c]	toluene	1.9978	8.8	–
	$(^nBu)_4N^+$	DMF [d]	2.0050	–	$a_Hp = 1.1$ (2H)
					$a_Ho = 1.0$ (4H)
					$a_Hm = 0.35$ (4H)
PPD	$MeCpMo(CO)_2$	toluene	1.9995	7.7	$a_HMe = 4.1$ (3H)
	$CpMo(CO)_2$ [c]	toluene	1.9987	7.6	$a_HMe = 4.2$ (3H)
					$a_Ho = 0.9$ (2H)
					$a_Hp = 0.8$ (1H)
					$a_Hm = 0.4$ (2H)
	K^+	DMSO/ ^{t}BuOH (4:1) [g]			$a_HMe = 3.43$ (3H)
					$a_Hp = 1.84$ (1H)
					$a_Ho = 1.59$ (2H)
					$a_Hm = 0.53$ (2H)
DA	$MeCpMo(CO)_2$	toluene	2.0007	6.2	$a_HMe = 5.7$ (6H)
	$CpMo(CO)_2$ [c]	toluene	1.9998	6.1	$a_HMe = 5.8$ (6H)
	K^+	DMSO [h]	2.00483	–	$a_HMe = 7.0$ (6H)
AQ	$MeCpMo(CO)_2$	toluene	2.0009	5.1	$a_H3,5,6,8 = 1.0$ (4H)
					$a_{13C} = 0.6$ (2C) [b]
	$CpMo(CO)_2$ [c]	toluene	2.0003	5.0	$a_H3,5,6,8 = 1.0$ (4H)
					$a_{13C} = 0.5$ (2C) [b]
	$(^nBu)_4N^+$	DMF [d]	2.0047	–	$a_H3,5,6,8 = 1.2$ (4H)
					$a_H4,7 = 0.25$ (2H)
	$MeCpMo(CO)_3$ [i]	toluene	2.0058	–	$a_H3,4,5,7 = 1.0$ (4H)
	$CpMo(CO)_3$ [f]	toluene	2.0055	–	$a_H3,4,5,7 = 1.1$ (4H)

---

[a] The number of equivalent protons is indicated in parentheses. [b] The hyperfine coupling constant of ^{13}C in carbon monoxide. The number of equivalent ^{13}C's is indicated in parentheses. [c] Reference 5. [d] The anion radical is produced by electrolytic reduction. [e] The data are for the precursor in which PQ coordinates to Mo by the C_{10}-oxygen. [f] Reference 11. PQ coordinates to Mo by the C_{10}-oxygen and AQ coordinates to Mo by the C_2-oxygen. [g] Reference 20. The values are for the radical having a *trans* C=O–C=O configuration. [h] Reference 21. [i] The data are for the precursor in which AQ coordinates to Mo by the C_2-oxygen.

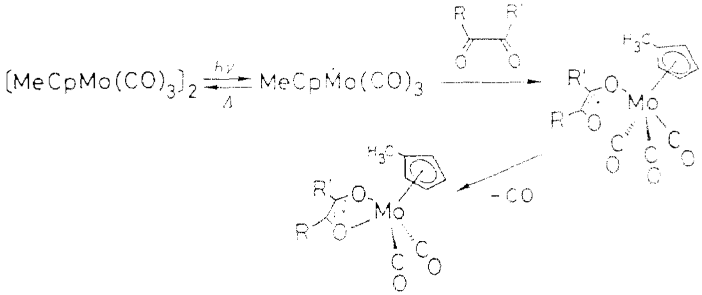

Scheme 1.

In the photochemical reactions of **2** with other quinones or with 1,2-diketones, formation of a similar type of paramagnetic chelate complexes was observed. The EPR parameters are listed in Table 1 together with those of the free anion radicals of the corresponding *o*-quinones and 1,2-diketones, and those of the complexes derived from **1** for comparison.

In the case of AQ and PQ, the complexes corresponding to the precursor of the chelate complex, MeCpMo(CO)$_3$(*o*-quinone), were observed during and immediately after photoirradiation at temperatures below $-40\,^{\circ}$C as was previously reported in the photochemical reaction of **1** with *o*-quinones (Table 1) [11]. The reaction mechanism, therefore, may be written as Scheme 1:

MeCpMo(CO)$_3$ formed by photocleavage of the Mo–Mo bond of **2** is trapped by the *o*-quinones or 1,2-diketones, and then the chelate complex is formed by the elimination of one of the CO groups from the precursor and the coordination of the other carbonyl group of the *o*-quinones or 1,2-diketones.

One of the most characteristic features of the paramagnetic chelate complexes produced is the remarkable changes of the g values and Mo hf coupling constants with *o*-quinone or 1,2-diketone ligands. A good correlation is seen between the changes in the g's and Mo hf couplings (Fig. 3). Similar changes in the g values and the Mo hf couplings have been observed also in the complexes of **1**. Such changes in the g values and Mo hf couplings as those observed here can be attributed to the changes of unpaired electron distribution between the metal moiety MeCpMo(CO)$_2^+$ and the quinone or diketone ligands [5].

One can see from Fig. 3 that the g values in the present system are larger than those of the corresponding complexes from **1** and closer to a free spin value ($g_e = 2.0023$), while the Mo hf coupling constants are a little larger in the present system. On the other hand, as shown in Table 1, the ^{13}C hf couplings increase and the quinone proton hf couplings decrease a little with the change from the complex system of **1** to **2**. Though the g value depends not only on the unpaired electron distribution in the complexes, but also on the excited configuration of electrons contributing to the orbital angular momentum, the hf coupling constants reflect directly the distribution of the unpaired electron in the complexes. So, one can see from the observed changes in the Mo, ^{13}C and quinone proton hf couplings that the spin density on the quinone is decreased by the substitution of methyl at the cyclopentadienyl ring, while that on the metal moiety is increased; the unpaired electron distribution drifts slightly from the quinone to the metal moiety.

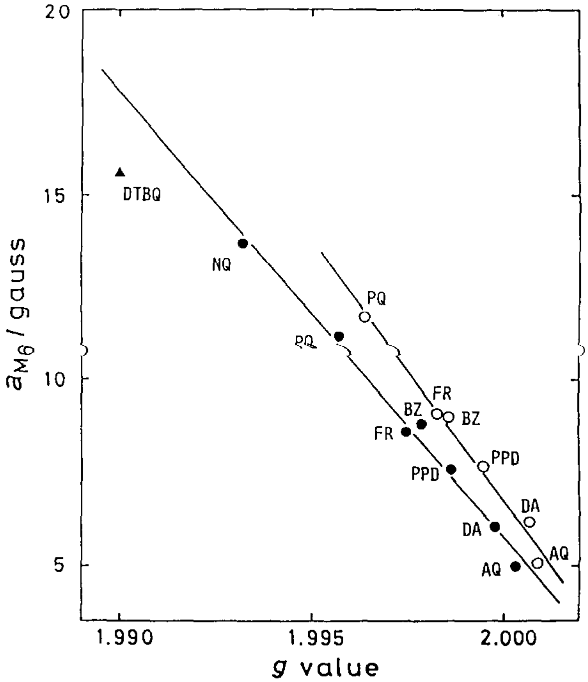

Fig. 3. Plots of a_{Mo}'s vs. *g* values of the complexes $MeCpMo(CO)_2$(o-quinone) (○), $CpMo(CO)_2$(*o*-quinone) (●), and $CpMo(CO)_2$(DTBQ) (▲). The data for $CpMo(CO)_2$(*o*-quinone) and $CpMo(CO)_2$(DTBQ) are taken from refs. 5 and 22, respectively (NQ = 1,2-naphthoquinone, DTBQ = 3,6-di-tert-butyl-1,2-benzoquinone).

According to the model proposed in the previous paper, the unpaired electron orbital, SOMO, is formed by the antibonding combination of the π type orbital in the metal moiety and the π LUMO of the quinones [5]. The spin distribution between the metal fragment and the quinone ligand depends on the relative energy heights of both the orbitals; the contribution of the metal moiety orbital to SOMO increases if its energy is elevated. Since the electron donative nature of the methyl substituted at the cyclopentadienyl ring would elevate the π type LUMO of the metal moiety, it is expected that this would increase the unpaired electron population on the metal moiety. This is in good agreement with the experimental results and it indicates also that the model proposed for the unpaired electron orbital is reasonable.

In addition to the changes in the distribution of unpaired electrons appreciable line width broadening is observed in the EPR spectra of the complex system of **2** as shown in Fig. 4. The signals with the symbol ★ are due to the complex derived from **1**, and those with symbol ○ to the complex from **2**. The latter signals show much larger line widths than the former. These line widths did not change with temperature and hence the broadening may not be due to relaxation processes arising from intramolecular motions such as the rotation of the cyclopentadienyl group. It may rather be due to the presence of some isomers in the complexes from **2** which differ in orientation of the methyl group of the cyclopentadienyl ring, i.e., the observed EPR spectra are the overlaps of isomers with slightly different EPR parameters.

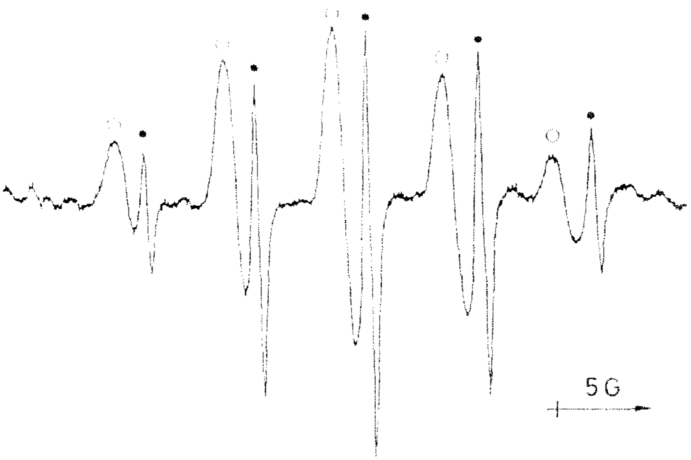

Fig. 4. First-derivative X-band EPR spectrum of a toluene solution containing MeCpMo(CO)$_2$(DA) (○) and CpMo(CO)$_2$(DA) (★) at −40 °C.

Photochemical reaction of 2 with p-benzoquinones

The photoirradiation of the toluene solutions of **2** in the presence of *p*-benzoquinones also gave EPR spectra, which showed ^{95,97}Mo hf couplings, proton hf couplings attributable to the *p*-benzoquinone ligand and also hf couplings due to the ^{13}C nuclei for the ^{13}CO enriched sample, **2′**. These EPR spectra indicate the formation of paramagnetic complexes as shown in Scheme 2. In the complexes, the *p*-benzoquinone coordinates as a monodentate ligand to the MeCpMo(CO)$_3$ produced by photocleavage of **2**. The EPR parameters obtained for the complexes are listed in Table 2 together with those of the complexes formed in the photochemical reactions of **1** with *p*-benzoquinones [6] for comparison. Main features of the spectra correspond well to those of the complexes from **1**, though in some cases one can see characteristic difference in the hf splittings due to ^{13}C's, i.e., in the BQ and 2,6-DMBQ complexes from **1**, the hf coupling constant of the two equivalent ^{13}C's is smaller than that of the other non-equivalent ^{13}C, while in the complexes from **2**, the former is larger than the latter.

The correlation between the ^{13}C hf couplings and molecular structures were examined by extended Hückel MO calculations for a model complex shown in Fig. 5. It was calculated that the spin distribution on the carbonyl groups changes very sensitively in response to changes of the Mo–O–C angle, and it may be one possibility that the Mo–O–C angle is slightly larger in the complexes from **2** than in the complexes from **1**.

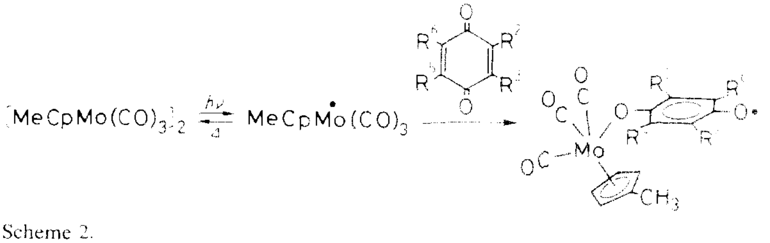

Scheme 2.

Table 2. EPR parameters for the paramagnetic complexes of $MeCpMo(CO)_3$ (*p*-benzoquinone) and $CpMo(CO)_3$ (*p*-benzoquinone) at −40 °C.

p-Benzoquinone	Metal	Solvent	*g*-value	a_{Mo}/G	a_H2/G	a_H3/G	a_H5/G	a_H6/G	a_{13C}/G [a]
BQ [b]	$MeCpMo(CO)_3$	toluene	2.0048	0.3	4.65	–	–	4.65	0.78(2C), 0.35(1C)
		THF	2.0048	0.4	4.53	0.22	0.22	4.53	0.73 (2C), 0.25 (1C)
		MTHF	2.0048	0.4	4.57	0.19	0.19	4.57	
	$CpMo(CO)_3$ [c]	toluene	2.0047	0.4	4.69	–	–	4.69	0.73 (1C), 0.38 (2C)
2-MBQ [b]	$MeCpMo(CO)_3$	toluene	2.0046	–	4.2 (Me)	0.3	0.3	4.7	
	$CpMo(CO)_3$ [c]	toluene	2.0045	0.3	4.2 (Me)	0.3	0.3	4.8	0.7 (1C), 0.3 (2C)
2,6-DMBQ [b]	$MeCpMo(CO)_3$	toluene	2.0045	0.1	4.20 (Me)	–	–	4.20 (Me)	0.65 (2C), 0.41 (1C)
		THF	2.0045	0.2	4.00 (Me)	0.13	0.13	4.00 (Me)	
		MTHF	2.0045	0.2	4.05 (Me)	–	–	4.05 (Me)	
	$CpMo(CO)_3$ [c]	toluene	2.0044	–	4.20 (Me)	–	–	4.20 (Me)	0.77 (1C), 0.29 (2C)
2,5-DMBQ [b]	$MeCpMo(CO)_3$	toluene	2.0044	–	5.23 (Me)	–	–	3.84	unresolved
	$CpMo(CO)_3$ [c]	toluene	2.0045	–	5.2 (Me)	0.4	–	3.7	unresolved
2,6-DTBQ [b]	$MeCpMo(CO)_3$	toluene	2.0044	0.3	–	–	–	–	0.5 (3C)
	$CpMo(CO)_3$ [c]	toluene	2.0044	0.4	–	–	–	–	1.0 (1C)
2,5-DTBQ [b]	$MeCpMo(CO)_3$	toluene	2.0043	–	–	–	–	4.18	1.13 (1C)
	$CpMo(CO)_3$ [c]	toluene	2.0045	0.7	–	–	–	4.07	1.10 (1C)
2-PBQ [d]	$MeCpMo(CO)_3$	toluene	2.0046	–	–	4.1	5.1	–	
	$CpMo(CO)_3$ [c]	toluene	2.0047	–	–	4.12	5.12	–	1.1 (1C), 0.6 (2C)
2-PBQ [b]	$MeCpMo(CO)_3$	toluene	2.0047	–	–	–	–	4.5	
	$CpMo(CO)_3$ [c]	toluene	2.0046	–	0.6 (*para*) 0.6 (*ortho*) 0.3 (*meta*)	–	–	4.45	unresolved
2,5-DPBQ [b]	$MeCpMo(CO)_3$	toluene	2.0045	–	–	–	–	3.87	
	$CpMo(CO)_3$ [c]	toluene	2.0047	–	0.7 (*para*) 0.7 (*ortho*) 0.3 (*meta*)	–	–	3.90	
TFBQ	$MeCpMo(CO)_3$	toluene	2.0052	–	10.0 (F)	1.6 (F)	1.6 (F)	10.0 (F)	
	$CpMo(CO)_3$ [c]	toluene	2.0052	–	10.0 (F)	1.7 (F)	1.7 (F)	10.0 (F)	
TCBQ [b]	$MeCpMo(CO)_3$	toluene	2.0062	2.8	–	–	–	–	
	$CpMo(CO)_3$ [c]	toluene	2.0063	3.2	–	–	–	–	

[a] The hyperfine coupling constants of ^{13}C's in carbon monoxide. The number of equivalent carbons is indicated in parentheses. [b] The EPR parameters for the complex in which the C_4-oxygen coordinates to Mo. [c] Reference 6. [d] The EPR parameters for the complex in which the C_1-oxygen coordinates to Mo.

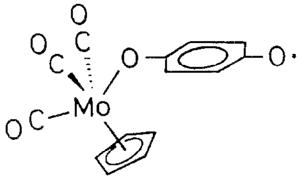

Fig. 5. The structure of the model complex for the extended Hückel MO calculations.

In contrast to what is observed with the chelate type complexes with *o*-quinones and 1,2-diketones, the *g* values and Mo hf couplings in the complexes of *p*-benzoquinones do not change so much with the quinone ligands. From comparison of the proton hf couplings with those of the free quinone anions, the most unpaired electron is considered to populate the quinone ligands, i.e., the unpaired electron populate mostly the π LUMO of the quinones, and there is no remarkable change of spin distribution between the complexes from **1** and **2**.

The coordination of the *p*-benzoquinone to the molybdenum is extensively affected by steric factors of the substituents adjoining the quinone carbonyl groups. For example, in the reactions with 2,6-dialkylsubstituted *p*-benzoquinones, the only complexes observed were those in which the molybdenum was coordinated by the C_4 carbonyl oxygen of the quinones. On the other hand, in the reaction with 2-PBQ, two type complexes were formed as shown in the EPR spectrum (Fig. 6); th EPR absorption showing a doublet of multiplets (○) is due to the complex in which the molybdenum is coordinated by the C_4 carbonyl oxygen, and the other showing a doublet of doublets (★) is due to the complex in which the molybdenum is coordinated by the C_1 oxygen. It can be easily seen that the formation of the former complex is much more highly favoured than the latter. Such selectivity in the coordination was also observed in the photochemical reactions of **1**. However, in the reaction of **1** with 2-PBQ, the relative ratio of the C_1 coordination type complex to the C_4 coordination type was 1/3 which is larger than the ratio in the case of **2**. This indicates that the steric factor more strongly affects complex formation in the reaction of **2** with *p*-benzoquinones.

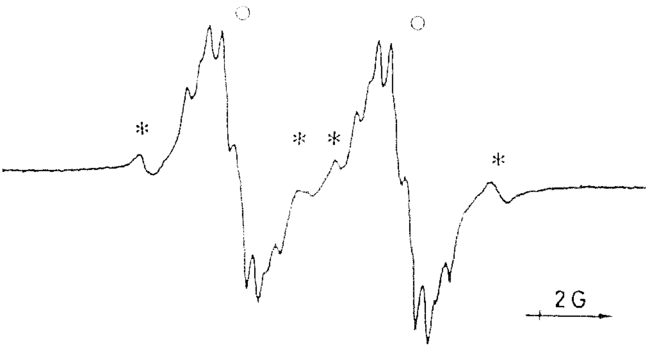

Fig. 6. First-derivative X-band EPR spectrum of a toluene solution of $MeCpMo(CO)_3(2\text{-}PBQ)$ at −40 °C. The signals marked with ○ are for the C_4-oxygen coordinating complex and the ones marked with ★ are for the C_1-coordinating complex.

The EPR spectrum observed for the BQ complex at $-40\,^{\circ}\mathrm{C}$ exhibits a triplet proton hf splitting, i.e., the hf coupling is symmetrical about the axis connecting the two carbonyl groups of the *p*-benzoquinone ligand (Table 2). However, by cooling the solution, the EPR spectrum began to show the line-width alternation effect and by cooling further it became a doublet of doublets pattern due to couplings with non-equivalent two protons (Fig. 7a) [12]. Such temperature variations of the EPR spectra were observed also for the 2,6-DMBQ complex (Fig. 7b), and they are attributed to restricted intramolecular motions.

Two types of motions are considered as possible causes for such effects. One is the rotation of the *p*-benzoquinone ligand about the C–O(–Mo) bond and the other is the rotation of the MeCpMo(CO)$_3$ group about the Mo–O bond. The similar line width alternation effect due to the restricted intramolecular motion has been reported for the monoprotonated *p*-benzosemiquinone radical and has been explained by the restricted rotation of the OH group about the C–O bond [13]. In view of this fact, it seems likely that the line width alternation effect observed in the present system is to be attributed to the restricted rotation of the *p*-benzoquinone ligand about the C–O(–Mo) bond. The most stable conformation of the complexes is considered to be the one where the Mo–O bond is in the benzoquinone plane. In such a conformation, the proton hf couplings cease to be symmetrical about the axis

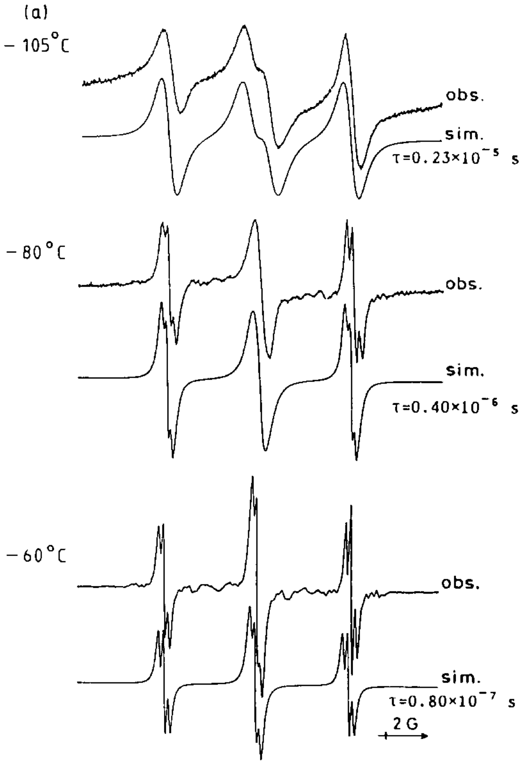

Fig. 7. First-derivative X-band EPR spectra of the complexes MeCpMo(CO)$_3$(BQ) in MTHF (a) and MeCpMo(CO)$_3$ (2,6-DMBQ) in MTHF (b) at different temperatures, and their simulated spectra calculated by use of modified Bloch equations assuming the two-jump model.

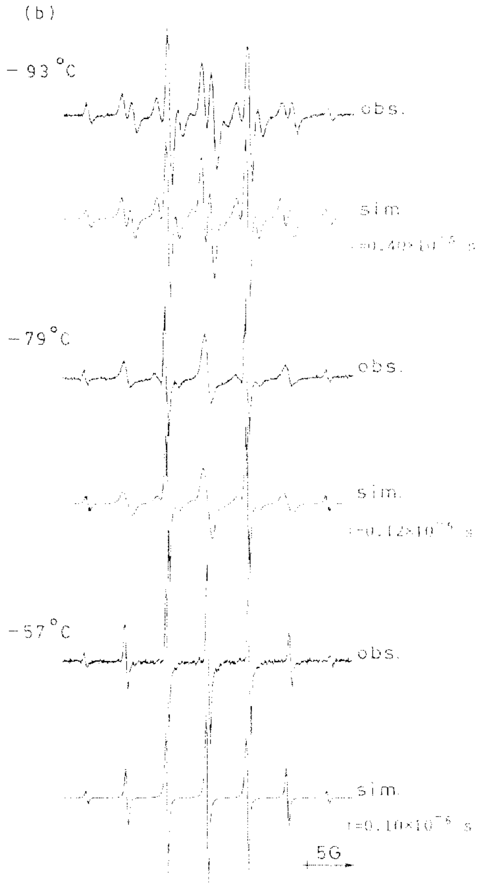

Fig. 7 (continued).

connecting the two carbonyl groups, and the π electrons of the benzoquinone can delocalize more onto the metal moiety.

The temperature dependent EPR spectra were analyzed by the modified Bloch equation for the restricted rotation of benzoquinone ligand assuming a two-jump model. The simulated spectra are shown in Figs. 7a and 7b with the observed spectra. From the plots of $\log_{10}(1/\tau)$ vs. $1/T$ (Fig. 8), the activation energies obtained for the restricted rotation in the BQ and 2,6-DMBQ complexes were 25 ± 2 kJ/mol and 29 ± 2 kJ/mol, respectively.

In the case of the complexes from **1**, this type of spectral change with temperature was observed only at temperatures near the freezing point of the solvent. This indicates that the methyl group in the cyclopentadienyl ring has an appreciable effect on the rotation of the *p*-benzoquinone ligand; the methyl group would make the transition state in the intramolecular motion unstable by steric interactions with other ligands, leading to higher activation energies for the complexes from **2** than those of the complexes from **1**.

The results obtained here imply that the EPR spectra recorded at high temperatures do not necessarily give information about the most stable structure for this

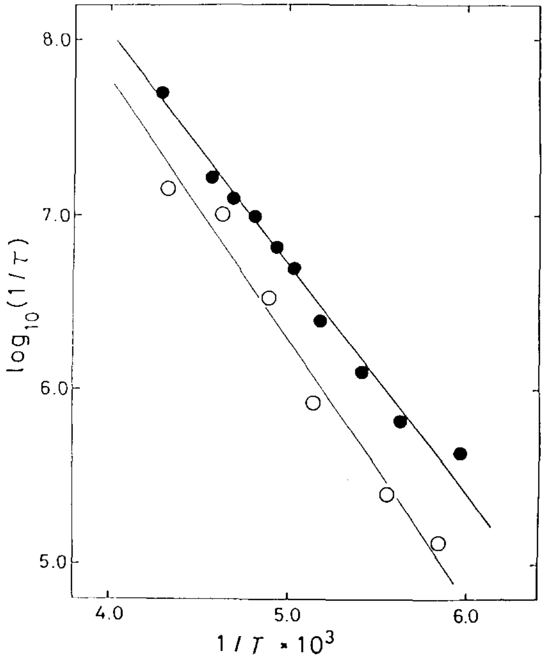

Fig. 8. Plots of $\log_{10}(1/\tau)$ (τ: correlation time/s) vs. $1/T$ (T: temperature/K) for the complexes of BQ (●) and 2,6-DMBQ (○).

kind of complex. It is known that *p*-benzoquinones coordinate to group 4B organometallic and also to some transition metals by one of the carbonyl oxygens producing paramagnetic complexes [14–19]. However, neither details of the coordination structures nor dynamic motion of the complexes have been known. This is the first case which shows clearly the most stable conformation of the *p*-benzoquinone ligands and their restricted rotation.

References

1 G.L. Geoffroy and M.S. Wrighton, Organometallic Photochemistry, Academic Press, New York, 1979.
2 G.L. Geoffroy, J. Chem. Educ., 60 (1983) 861.
3 T.J. Meyer and J.V. Caspar, Chem. Rev., 85 (1985) 187.
4 A.E. Stiegman and D.R. Tyler, Coord. Chem. Rev., 63 (1985) 217.
5 M. Hanaya, S. Tero-Kubota and M. Iwaizumi, Organometallics, 7 (1988) 1500.
6 M. Hanaya and M. Iwaizumi, Organometallics, 8 (1989) 672.
7 D.S. Ginley, C.R. Bock and M.S. Wrighton, Inorg. Chim. Acta, 23 (1977) 85.
8 J.L. Hughey, C.R. Bock and T.J. Meyer, J. Am. Chem. Soc., 97 (1975) 4440.
9 D.S. Ginley and M.S. Wrighton, J. Am. Chem. Soc., 97 (1975) 3533.
10 N.N. Turaki and J.M. Huggins, Organometallics, 4 (1985) 1766.
11 M. Hanaya and M. Iwaizumi, Bull. Chem. Soc. Jpn., 63 (1990) 275.
12 Preliminary results about the line width alternation effect have been previously reported as a short communication: M. Hanaya and M. Iwaizumi, Chem. Lett., (1989) 1381.
13 T.E. Gough, Can. J. Chem., 47 (1969) 331.
14 A. Albert and A. Hudson, J. Chem. Soc., Perkin Trans. 2, (1978) 1098.
15 K.S. Chen, T. Foster and J.K.S.T. Wan, J. Chem. Soc., Perkin Trans. 2, (1979) 1288.
16 A. Vlcek Jr., J. Klima and A.A. Vlcek, Inorg. Chim. Acta, 58 (1982) 75.

17 A. Vlcek Jr., J. Klima and A.A. Vlcek, Inorg. Chim. Acta, 69 (1983) 191.

18 J.-P.M. Tuchagues and D.N. Hendrickson, Inorg. Chem., 22 (1983) 2545.

19 A. Vlcek Jr., J. Organomet. Chem., 297 (1985) 43.

20 G.A. Russell, E. Thomas Strom, E.R. Talaty and S.A. Weiner, J. Am. Chem. Soc., 88 (1966) 1998.

21 G.A. Russell, D.F. Lawson, H.L Malkus, R.D. Stephens, G.R. Underwood, T. Takano and V. Malatesta, J. Am. Chem. Soc., 96 (1974) 5830.

22 K. Sarbasov, S.P. Solodovnikov, and B.L. Tumanskii, N.N. Bubnov and A.I. Prokofev, Izv. Akad. Nauk SSSR, Ser. Khim., (1982) 1509.